Bulletin of the Seismological Society of America, Vol. 79, No. 2, pp. 282–296, April 1989

SURFACE RUPTURES ON CROSS-FAULTS IN THE 24 NOVEMBER 1987 SUPERSTITION HILLS, CALIFORNIA, EARTHQUAKE SEQUENCE

BY K. HUDNUT, L. SEEBER, T. ROCKWELL, J. GOODMACHER, R. KLINGER, S. LINDVALL, AND R. MCELWAIN

ABSTRACT

Left-lateral slip occurred on individual surface breaks along northeast-trending faults associated with the 24 November 1987 earthquake sequence in the Superstition Hills, Imperial Valley, California. This sequence included the M_s = 6.2 event on a left-lateral, northeast-trending "cross-fault" between the Superstition Hills fault (SHF) and Brawley seismic zone, which was spatially associated with the left-lateral surface breaks. Six distinct subparallel cross-faults broke at the surface, with rupture lengths ranging from about $1\frac{1}{2}$ to 10 km and maximum displacements ranging from 30 to 130 mm. About half a day after the M_s = 6.2 event, an M_s = 6.6 earthquake nucleated near the intersection of the cross-faults with the SHF, and rupture propagated southeast along the SHF. Whereas right-lateral slip on the SHF occurred dominantly on a single trace in a narrow zone, the cross-fault surface slip was distributed over several stands across a 10-km-wide zone. Also, whereas afterslip accounted for a large proportion of total slip on the SHF, there is no evidence for afterslip on the cross-faults. We present documentation of these surface ruptures. A simple mechanical model of faulting illustrates how the foreshock sequence may have triggered the main rupture. Displacement on other cross-faults could trigger an event on the southern San Andreas fault by a similar mechanism in the future.

INTRODUCTION

Faults that trend northeast between bounding northwest-trending faults with right-lateral slip are important tectonic elements of the Salton trough. It has recently been found that these faults, here termed "cross-faults," are dominantly strike-slip faults with left-lateral motion. This implies that the present kinematic role of these faults is different than that proposed by studies that have considered these normal faults. Seismic ruptures of these faults also can be followed by larger ruptures on the main bounding faults, as seen in the Superstition Hills sequence. This sequence provided the first example on these cross-faults of surface ruptures; we document these with mapping and data analysis.

The Imperial Valley historically has been one of the most seismically active regions in California. Located near the southern termini of the San Andreas fault and San Jacinto fault zones, it is a region of tectonic transition from the Gulf of California "ocean rifting" regime to the southern California "continental transform" regime. The Brawley seismic zone, between the San Andreas fault and Imperial fault, is generally considered the northernmost ridge segment of the ridge/transform system in the Gulf of California (Lomnitz *et al.*, 1970). Detailed studies (Johnson and Hutton, 1982; Fuis *et al.*, 1984) show a complex structure, however, and the mechanism by which spreading is taking place in the Salton trough remains controversial.

Within this region, some of the prominent and seismically active faults trend northeast, roughly perpendicular to the strike of the main bounding faults (Fig. 1). These cross-faults are oriented normal to the inferred spreading direction, and were thought in some cases to be normal faults (Fuis *et al.*, 1984). A large aftershock of

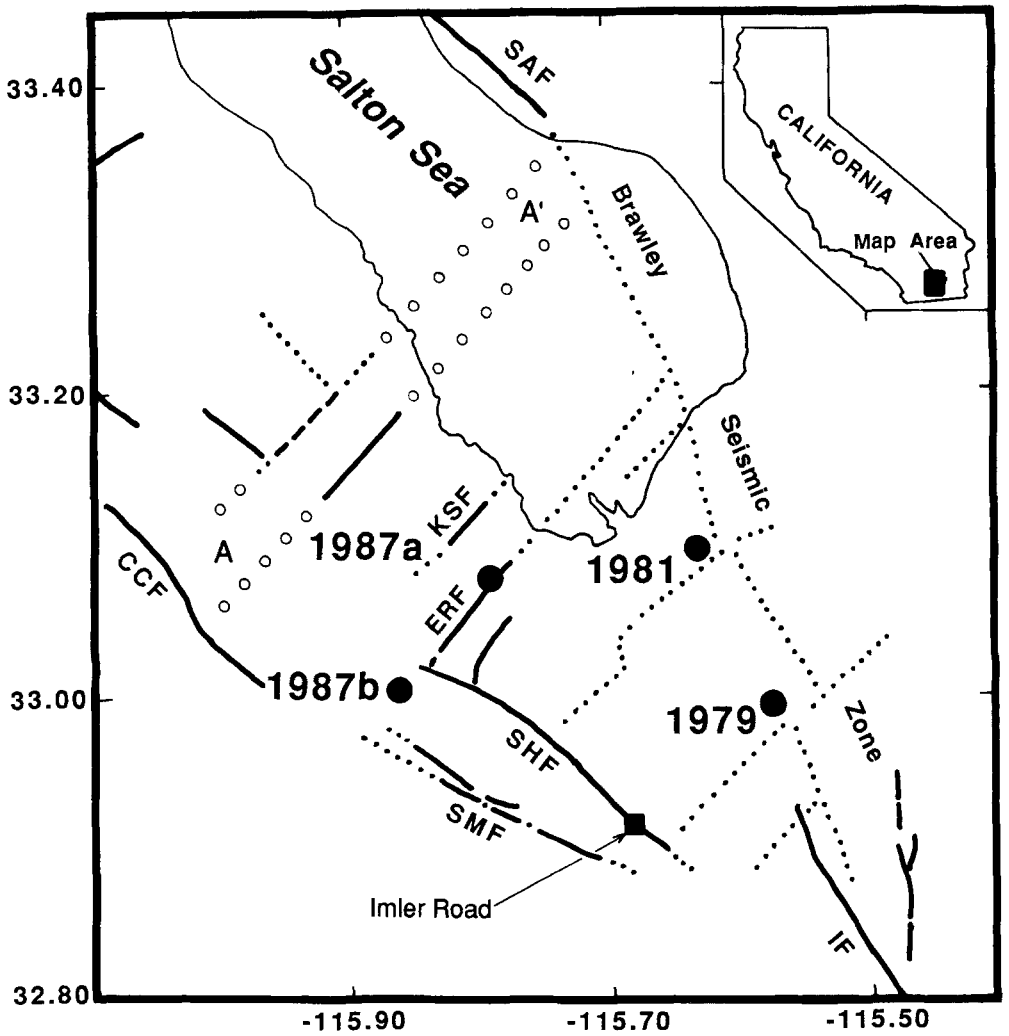

FIG. 1. Major known faults, faults inferred from seismicity (dotted lines), incompletely mapped (dashed lines), and inferred (open circles) in the region between the southern termini of the San Andreas fault and San Jacinto fault zone, including the Brawley seismic zone. Fault names are abbreviated as follows: SAF, San Andreas fault; IF, Imperial fault; CCF, Coyote Creek fault; KSF, Kane Spring fault; and ERF, Elmore Ranch fault. Epicenters related to the cross-fault rupturing 1979 aftershock and 1981 Westmorland event, and the two large earthquakes that occurred in November 1987 are shown. Aftershocks show the 1987 rupture of the ERF extended from the SHF to the Brawley seismic zone. Note the zone of cross-faults northwest of the Superstition Hills, labelled A-A′, that we name the Extra fault zone. Inset map shows the location of this study area in California.

the 1979 Imperial Valley earthquake (Johnson and Hutton, 1982), and the main shock of the 1981 Westmorland earthquake (Nicholson *et al.*, 1986) instead showed focal mechanisms indicating dominantly left-lateral slip. Seismological study of cross-fault events in the November 1987 sequence again showed left-lateral slip. Surface rupture on cross-faults in that sequence yields the first unambiguous geological evidence that the predominant present-day movement on these cross-faults is left-lateral strike-slip. Basement morphology (Fuis *et al.*, 1984) suggests dip-slip motion may have dominated in the past. The present-day kinematic role of the cross-faults remains unresolved.

The November 1987 Superstition Hills Sequence

Seismicity

The first large event, M_s = 6.2, occurred at 0154 on 24 November 1987 (GMT) and was co-located with several foreshocks of its own about 10 km northeast of the Superstition Hills fault (Fig. 2). Epicenters during the 10 hr following the Elmore Ranch earthquake (M_s = 6.2) showed a northeast trend extending from the Superstition Hills fault to the Brawley seismic zone (L. Jones and D. Given, personal comm., 1987). Early epicentral locations from the CIT/USGS network guided our efforts during the surface rupture mapping. Subsequent relocations of these earthquakes confirmed that the rupture was on a northeast-trending fault zone (Magistrale *et al.*, 1989). Aftershock patterns indicate that this event probably propagated bilaterally to the northeast, to the Brawley seismic zone, and to the southwest, toward its zone of intersection with the northwestern end of the Superstition Hills fault surface rupture.

At 1315 on 24 November the main shock of the sequence (M_s = 6.6) occurred. Within location errors, this event was located close to the northwestern terminus of the SHF, near its intersection with the Elmore Ranch fault surface rupture zone. Aftershock locations of this event formed a northwest-southeast trending zone, roughly paralleling the Superstition Hills fault, but several kilometers southwest of the surface trace of the fault, and concentrated near the intersection of the cross-faults with the SHF.

Surface-Rupture Chronology

At 1030 (GMT) on 24 November no new surface rupture was observed on the Superstition Hills fault at Imler Road (Fig. 1) following the Elmore Ranch earthquake, but rupture was observed on the SHF half an hour following the main event (Kahle *et al.*, 1988). Unfortunately, no northeast-trending surface ruptures were observed until after the main shock had already occurred. Thus, while the temporal correlation between the main shock on the SHF and its related surface rupture is strong, such a correlation for the Elmore Ranch event is uncertain.

Significant afterslip on the SHF was observed shortly after the main earthquake; afterslip is continuing (at much slower than initial rates) as of October 1988. Slip on the main fault surface ruptures are approaching 90 cm, including afterslip, along some parts of the fault (Sharp *et al.*, 1989; Williams and Magistrale, 1989). We found no evidence for afterslip on any of the cross-faults. Small amounts of surface slip, possibly triggered, were observed on parts of both the Imperial fault (Sharp, 1989; McGill *et al.*, 1989) and the Coyote Creek fault (Hudnut and Clark, 1989).

The set of northeast-trending, left-lateral fault breaks (Fig. 2) nearly parallel the trend of the foreshock sequence epicenters (Magistrale *et al.*, 1989). The seismic moment of the largest foreshock is in the size range for which surface ruptures usually occur in California. There were no field observations on these faults between the times of the foreshock sequence and main shock. Despite this caveat, we associate the cross-fault surface ruptures with the foreshock sequence.

Methods

Displacements were measured across features such as the edges of fractures, tire tracks, and linear features on the soil surface that could be matched reliably on either side of the fault. Care was taken that the along-strike component of strike-slip was measured. In some instances, dip slip and extension across the cracks were

also measured. Most measurements were across single fault strands, though some were made over multiple strands at a single site. Most offset determinations represent the largest offset of several measurements at one locality, though usually the slip was consistent at each locality. All of the fault breaks we mapped were examined on foot for their entire lengths. Deviation from even sampling along the faults usually was because of ground shattering, or otherwise nontectonic slumping that obscured the rupture trace. Many, but not all, offset features were documented with photographs. Aerial photographs were used as base maps for plotting surface faulting in the field, and final data transfer from the field photos to $7\frac{1}{2}$ min topographic quadrangles was done using a zoom transfer scope.

A WILD® TC-2000 surveying instrument was used to obtain accurate locations of the mapped faults and displacement measurement sites. The instrument was used for spot-checking mapping done soon after the earthquakes, and for station locations concurrent with field mapping later on. We field checked much of our mapping with the instrument. The instrument was most useful for correcting mapping discrepancies, and for removing the distortion inherent in airphoto-based mapping.

Our afterslip markers were spray-painted lines and tire tracks. We have especially monitored the Kane Spring fault and Elmore Ranch fault (Fig. 2), through October 1988. Beginning in March 1988, slip on the Elmore Ranch fault has been monitored with alinement arrays.

Cross-Fault Surface Ruptures

Description

All of the 1987 surface ruptures were on pre-existing faults displacing consolidated and deformed strata of the Pleistocene Brawley Formation. Moreover, in places these faults exhibit geomorphic expression of prior slip such as scarps, en-echelon folds (forming subtle topographic highs), and linear ridges or sags. The majority of surface ruptures were confined to faults that had been previously mapped along at least part of their lengths (Dibblee, 1984; unpublished maps by Sharp and Lienkaemper, and by Hudnut). Several of the previously mapped faults in this area did not show surface slip in this earthquake sequence, while some ruptures occurred on previously unmapped faults. Although their past slip orientations may have been different, the 1987 surface rupture shows these northeast-trending faults are all dominantly left-lateral faults.

Names used here (see Fig. 2) for each of the six fault strands that ruptured are, from southeast to northwest, the Lone Tree fault (after Lone Tree Wash), the Eastern, Central, and Western Elmore Ranch faults (after Elmore Desert Ranch), and the Eastern and main Kane Spring faults (after Kane Spring). Cracking and possibly minor slip was also noted on the Extra fault (after benchmark EXTRA; fault zone is labelled A-A′ in Fig. 1) to the northwest of the Kane Springs fault. The three strands of the Elmore Ranch fault were treated as a single fault zone because each of the strands either joins or branches from the central strand somewhere along the length of their ruptures (Fig. 2).

The cross-fault surface ruptures typically consisted of short en-echelon breaks that in places stepped to the left or right, producing small areas of extension or shortening. Some of the rupture segments, particularly those associated with larger amounts of surface slip on strands of the ERF zone did exhibit continuous breaks for tens to hundreds of meters long.

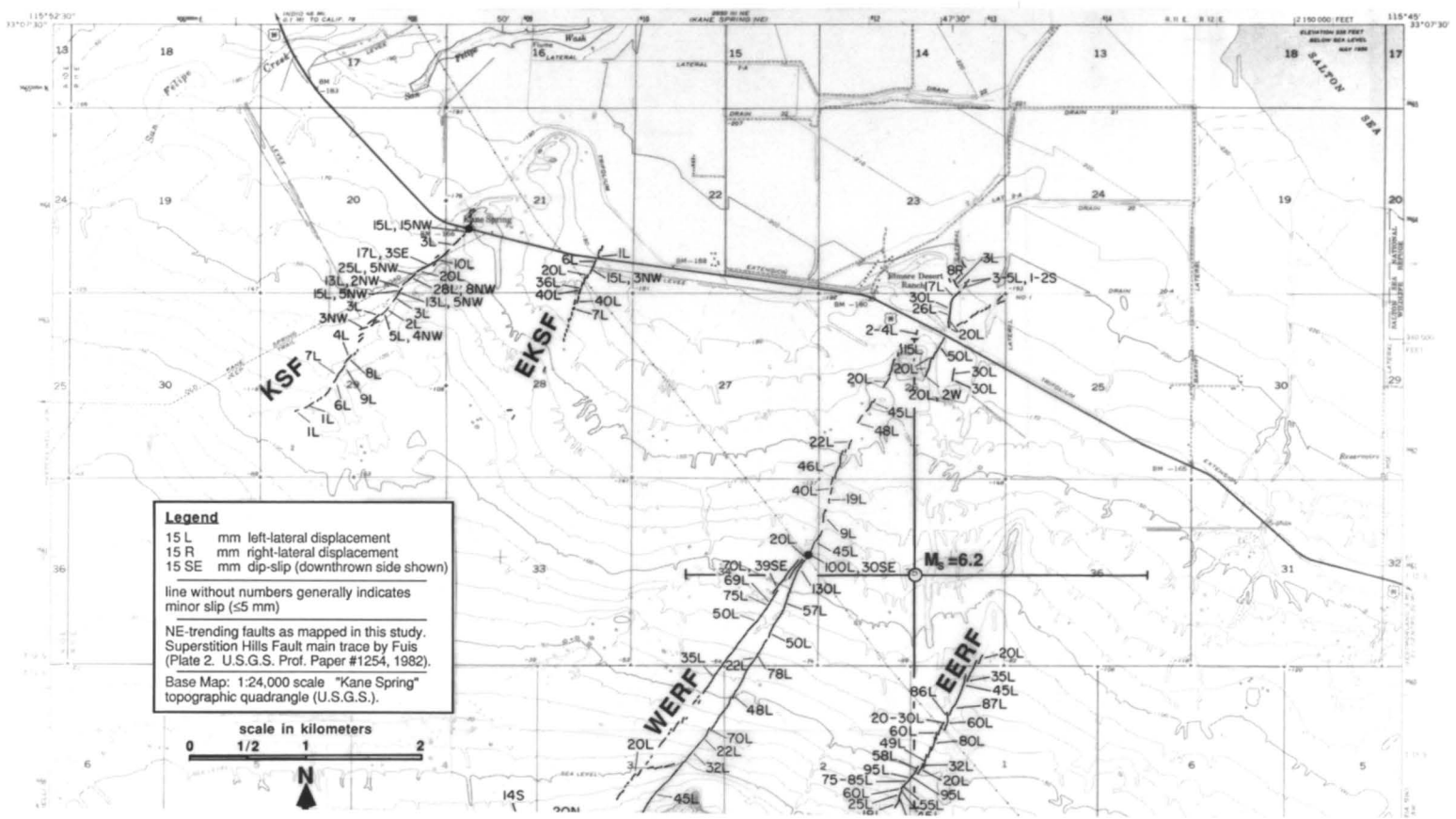
KSF
EKSF
WERF
EERF
M_s=6.2
Legend
15 L mm left-lateral displacement
15 R mm right-lateral displacement
15 SE mm dip-slip (downthrown side shown)
line without numbers generally indicates minor slip (≤5 mm)
NE-trending faults as mapped in this study. Superstition Hills Fault main trace by Fuis (Plate 2. U.S.G.S. Prof. Paper #1254, 1982).
Base Map: 1:24,000 scale "Kane Spring" topographic quadrangle (U.S.G.S.).
scale in kilometers
0 1/2 1 2
N
Kane Spring
Wash
SALTON SEA

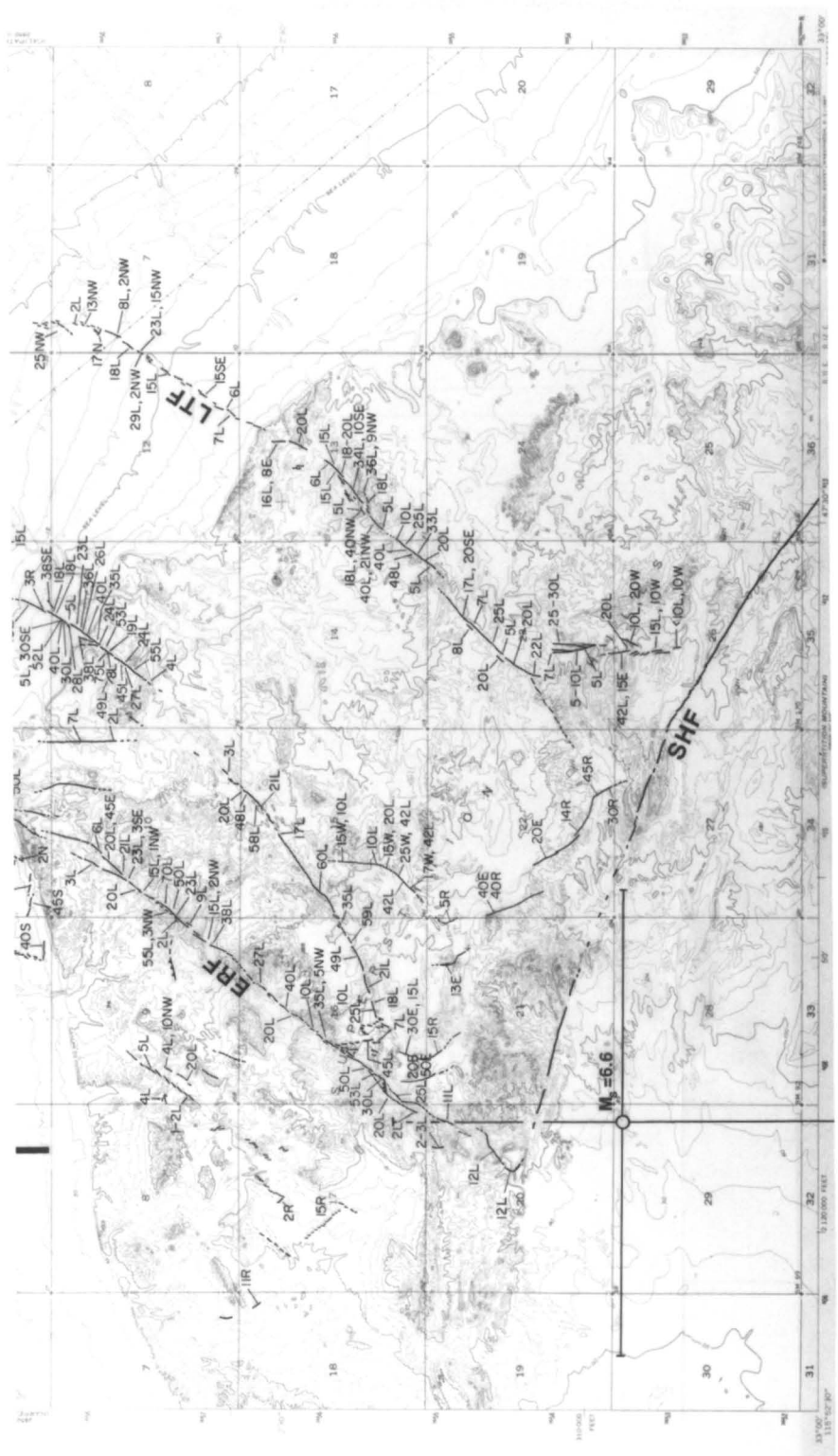
LTF
ERF
SHF
M_L=6.6

FIG. 2. Map of surface ruptures along cross-faults and surface slip data, also showing proposed names for the cross-faults. The names are: KSF, Kane Spring fault; EKSF, Eastern Kane Spring fault; WERF, Western Elmore Ranch fault; ERF, Elmore Ranch fault; EERF, Eastern Elmore Ranch fault; LTF, Lone Tree fault. Epicenters of the largest events in the November 24, 1987 Superstition Hills earthquake sequence are shown, with ±2 km error bars (our estimate of the absolute location error). Base map is the Kane Spring ($7\frac{1}{2}$ minute topographic) quadrangle. Minor ruptures occurred on the Harper's Well quadrangle to the west. A map of these breaks, full-scale copies of the Kane Spring quadrangle mapping, and a key map to station locations with accompanying data listings, are available from the authors by request. Filled circles on the Kane Spring fault at the highway, and Elmore Ranch fault at the power line road, are stations where no afterslip has yet been observed.

Figures 3a and 3b show that cumulative displacement over multiple strands of the Elmore Ranch fault zone was up to nearly 200 mm of left-lateral slip. The main strand had up to 130 mm, the western strand had a maximum of 75 mm, and the eastern strand had as much as 95 mm of left-lateral slip. The Lone Tree, Kane Springs, and Eastern Kane Springs faults had maximum left-lateral displacements at the surface of 48, 28, and 40 mm, respectively. Maximum surface displacements on the Elmore Ranch fault strands occurred a few kilometers southwest of the epicentral location for the Elmore Ranch earthquake, whereas slip maxima on the Kane Spring strands were within a kilometer of the epicenter as projected onto the distance axes in Figure 3.

Terminations of Cross-Fault Breaks

At their northeastern ends, surface breaks on the Kane Spring fault, Elmore Ranch fault, Eastern Elmore Ranch fault, and Lone Tree fault terminated at fault bends and/or step-overs associated with anticlines. At their southwestern ends, near their intersections with the Superstition Hills fault, surface breaks on both the Elmore Ranch fault zone and the Lone Tree fault splayed into multiple strands. Surface breaks on the Elmore Ranch fault followed a nearly straight course to within a short distance of its intersection with the Superstition Hills fault. Left-lateral slip decreased to a few millimeters within 100 m of the intersection. Some of the slip apparently was distributed on nearly north-south trending normal faults (in the eastern quadrant of the fault intersection); displacement was down on the east side, with up to 50 mm of dip slip. These normal faults are arcuate in map view, concave eastward, with multiple splays. A component of left-lateral slip occurred on the northeast-striking splays, and a component of right-lateral slip occurred on the southeast-striking splays. Splays of these dominantly normal faults merged into right-lateral faults paralleling the Superstition Hills fault.

In contrast, the main surface break on the Lone Tree fault did not maintain a straight trend toward its intersection with the Superstition Hills fault. At a distance of about one kilometer northeast of the intersection, the northeast trend of surface breaks on the Lone Tree fault changed into a nearly north-south trend. The point of change in trend of the surface trace roughly coincides with the north-dipping limb of a major anticline. A minor break, with cracking but no measurable offset, splayed from this point towards the west, along the limb of the fold. The main break continued towards the Superstition Hills fault, showing dominantly left-lateral slip, and terminated near a fault that parallels the Superstition Hills fault, but did not rupture in the 1987 sequence.

MOMENT CALCULATIONS

Most surface ruptures on the cross-faults showed highly variable slip along-strike (Fig. 3a). In other well-studied examples of nearby earthquakes, slip versus distance

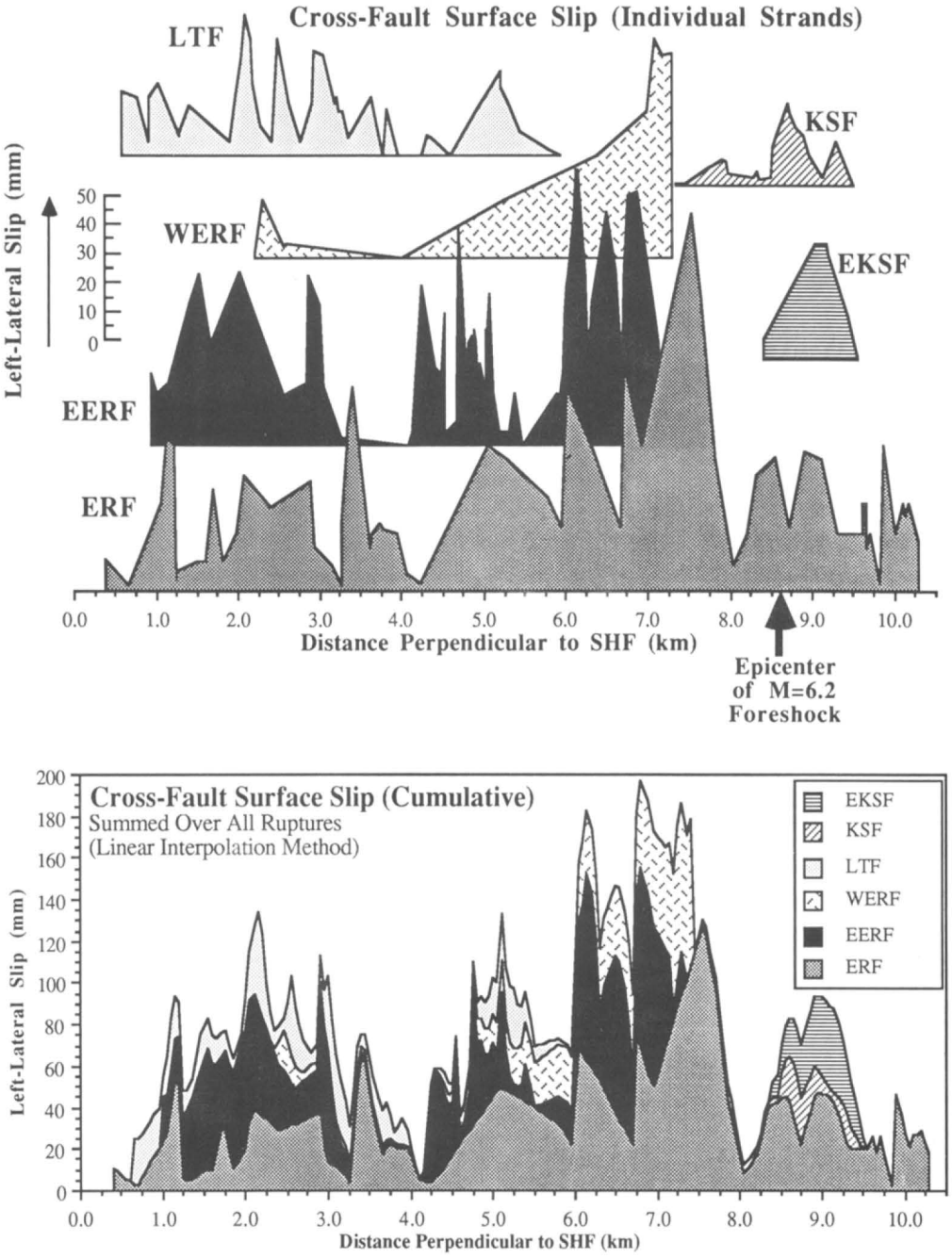

FIG. 3. a) Uninterpolated slip distribution curves (raw data) for each of the individual northeast-trending strands. b) Interpolated data (resampled at 50 m intervals), summed across all strands, i.e., total or cumulative slip distribution curves.

curves also appear jagged, as in the 1968 Borrego Mountain earthquake (Clark, 1972) and the 1979 Imperial Valley earthquake (Sharp *et al.*, 1982). We have calculated moment as directly as possible from the surface-slip data.

Raw surface rupture data (Fig. 3a) were first linearly interpolated, with a sampling interval of 0.01 km. Integration of the resulting series was computed using the

trapezoidal rule, to obtain the values in Table 1 (column $L \times x$) that were used in computing M_o for individual fault strands. The series were next decimated to a sampling interval of 0.05 km and then summed (Fig. 3b). Zero-phase low-pass filtering procedures were applied, but the smoothed curves (not shown) obscure details that we feel could be important, and were found to be less informative than Figure 3b. Complexity and splaying of the fault strands was not corrected for, so plots represent data from ruptures striking about N35 ± 10°E. Because of strike variations, some distortion (up to about 20 per cent of shown values) is present.

It is tempting to approach moment calculations based on surface slip by smoothing or averaging the surface-slip distribution curve, and claiming this more realistically represents slip at depth. Calculation of moment from distorted, smoothed, or simply averaged (over data sampled unevenly with distance) surface-rupture data does not accurately represent the field data and, depending on the methods used, may cause large errors. The method used here improves upon previous methods of calculating moment from surface-slip data on multiple parallel strands, but sparse data in places limits the accuracy of any technique one might use.

The total moment we calculated from the surface rupture data, 2.3×10^{24} dyne × cm (Table 1) is nearly an order of magnitude less than the moment obtained from teleseismic body waves for the largest foreshock ($M_s = 6.2$) of 1.8×10^{25} dyne × cm (Bent *et al.*, 1988). In our calculation, we assumed that μ (rigidity) = 3×10^{11} dynes/cm^2, and that rupture depth was 10 km, as constrained by the depth of most cross-fault seismicity (Magistrale *et al.*, 1989). Even if one were to assume 200 mm of left-lateral slip on a 10 km long break, this maximum estimate of moment from surface ruptures would be only 6 × 10 dyne × cm. There is also a discrepancy between rupture length determined by cross-fault seismicity of about 20 to 25 km, and that determined by surface rupture of about 10 km. These discrepancies may occur because rupture did not fully propagate to the surface.

Comparison to Other Earthquakes

These surface ruptures indicate differences in behavior between cross-faults and the main northwest-trending faults. Parallel faults spaced kilometers apart broke as a set in this sequence, with displacements on surface breaks distributed over a northeast-trending zone about 10 km wide and 10 km long. In contrast, ruptures on right-lateral faults such as the 1968 rupture of the Coyote Creek fault, the 1979 rupture of the Imperial fault, and the 24 November 1987 rupture of the SHF all occurred within narrower zones, usually of a kilometer or less wide, or even on a single strand.

In Table 1, we reduced the surface rupture data from each of the fault strands to the several quantities that have been commonly used to describe surface ruptures, as in Bonilla and Buchanan (1970), Slemmons (1977), and Scholz (1982). For the six discrete ruptures we studied, we compared fault length to both maximum slip (Fig. 4a) and mean slip (Fig. 4b).

Some consistency is seen in these comparisons; maximum and mean slip both increase with rupture length. Scholz (1982) points out that the physical basis for linear scaling between mean slip and fault length is that the proportionality constant, α, is proportional to stress drop, thus to friction on the fault surface. The value he obtained for large strike-slip events is $\approx 1.25 \times 10^{-5}$, whereas from our data alone we obtain $\alpha = 0.3 \times 10^{-5}$, but the line is poorly constrained and the values are not directly comparable. Without additional data from surface faulting or other

TABLE 1

SURFACE RUPTURE QUANTITIES AND MOMENT ESTIMATES

Fault	L (km)	Max. Slip (mm)	Mean Slip (mm)	$L \times x$ (m^2)	M_o (dyne×cm)
ERF	9.96	130	34.8	346.6	1.04×10^{24}
EERF	6.34	95	31.4	198.8	* 5.96×10^{23}
WERF	5.40	75	18.1	97.8	* 2.93×10^{23}
LTF	5.49	48	13.2	72.4	* 2.17×10^{23}
EKSF	1.44	40	20.0	28.8	* 8.64×10^{22}
KSF	2.16	28	8.3	17.9	* 5.37×10^{22}
Total				762.3	2.29×10^{24}

L = mapped surface rupture length.

$L \times x$ = Length times surface slip, obtained by integration using the trapezoidal rule on linearly interpolated data, sampled at 10 m intervals, using zero as the integration constant.

M_o = Moment, calculated from surface rupture data using the standard relation $M_o = \mu(L \times D)x$, where μ is rigidity (assumed to be 3.0×10^{11} dyne/cm^2), L is length of rupture plane, D is depth of rupture plane (assumed to be 10 km), and x is surface slip. Here, the quantity $L \times x$ is obtained by integration.

* Surface ruptures with $L/D \ll 1$, for which moment calculations are dominated by the assumed dimension D.

methods, one cannot yet reliably infer differences in friction between main faults and cross-faults.

CROSS-FAULT RUPTURE TIMING

The relation between major ruptures as defined by seismicity in the Superstition Hills sequence and by surface ruptures is complex in both space and time. It may be that not all of the cross-fault surface slip coincided with the Elmore Ranch event; some may have been associated with aftershocks in the ensuing ~11.4 hours, or caused by the main shock on the Superstition Hills fault. Lack of surface rupture observations immediately following the Elmore Ranch earthquake leave many questions regarding the temporal sequence of surface rupture unresolved. In one way, the temporal behavior of the northwest- and northeast-trending faults clearly differs; a significant portion of the total slip on the SHF has occurred as afterslip. In contrast, no afterslip has been detected on any of the northeast-trending surface ruptures since the evening of 24 November when some of the first afterslip markers were put out. Perhaps relevant to this lack of observed afterslip, seismicity on the cross-faults reportedly decreased substantially after the main rupture on the SHF occurred (H. Magistrale and K. Hutton, personal comm., 1988).

DISCUSSION

Some implications of the data warrant discussion as follows:

1. Cross-Fault Triggering. Northwest of the intersection between the cross-faults and SHF, no surface slip was observed on the SHF. The main event (M_S = 6.6) epicenter is located slightly southeast of the ERF intersection; the main shock rupture propagated towards the southeast from the intersection. We suggest that the main shock on the Superstition Hills fault was triggered primarily by the rapid decrease in normal stress across the Superstition Hills fault caused by the left-lateral displacement on the cross fault, which locally weakened the SHF (Fig. 5). The cross-fault rupture presumably also caused increased normal stress to the

northwest of the faults' intersection, thereby inhibiting bilateral rupture to the northwest. These concepts are developed further in Hudnut *et al.* (1989).

2. Potential Cross-Fault Triggering of the San Andreas Fault. Future slip on other known cross-faults would decrease normal stress across the southern San Andreas fault, potentially triggering an earthquake there by a mechanism similar to that observed in the Superstition Hills sequence. Other cross-faults are mapped northwest of the ERF; these form the Extra fault zone, labelled A-A′ in Fig. 1. Identification and mapping of these and other cross-faults that could trigger larger future earthquakes may help to evaluate whether hypocenters in a potential foreshock sequence are on a mapped cross-fault. Recognition of this mechanism should be helpful in developing a basis for prediction of earthquakes on the San Andreas fault.

Dibblee (1984) mapped a portion of the Extra fault in the eastern San Felipe

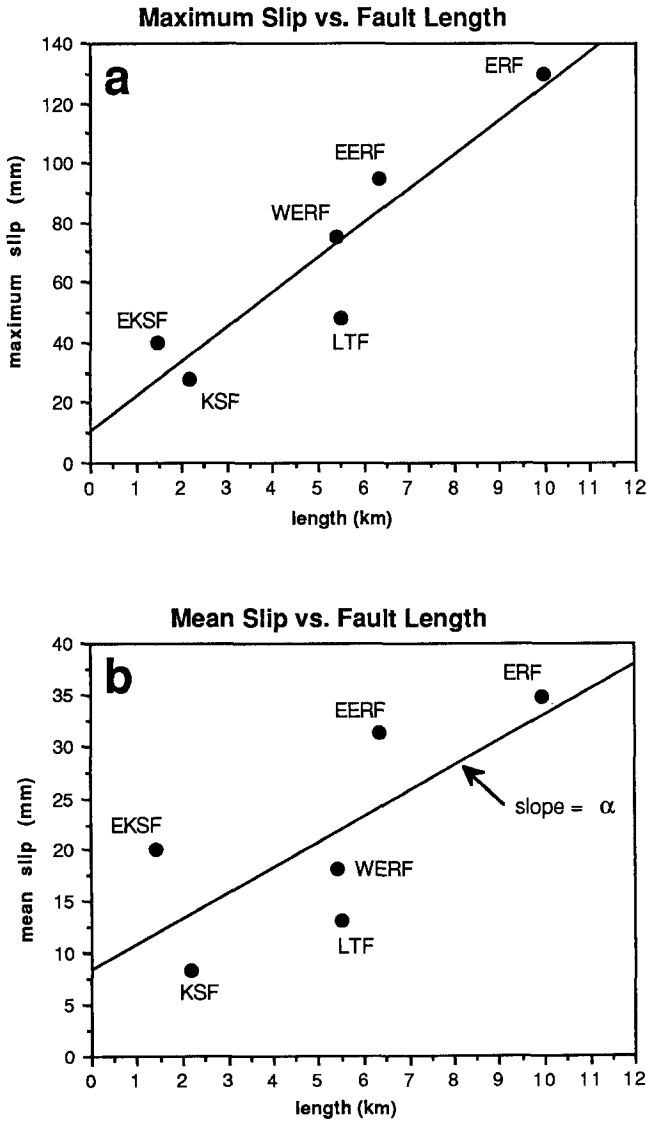

FIG. 4. Relations of quantities typically used to describe surface rupture. a) Maximum slip versus fault length. b) Mean slip versus fault length. Using Scholz (1982) equation; $\mu = \alpha L$, we determine $\alpha = 0.3 \times 10^{-5}$ from the poor linear fit to these data (see text).

Hills between highways 78 and 86, and further mapping has been done by Sharp (1981; personal comm., 1988), and recently by authors of this paper. The fault is associated at the surface with a northeast-trending linear concentration of roughly en-echelon anticlines, as is observed along the Kane Spring and Elmore Ranch faults. Along this fault, the belt of anticlines is mappable along strike for about 10 km through the eastern San Felipe Hills. Between anticlines, where the fault is best expressed, the fault trace offsets Pleistocene strata. Good exposures of the fault are seen in the deeper dry stream channels. Towards the southwest from this area, the fault is covered by sand dunes and alluvium, but a strong lineament is seen on airphotos and satellite images, extending the fault close to the Coyote Creek fault.

Toward the northeast, the fault is expressed by bathymetric contours in the Salton Sea, by a weak seismicity cluster along the Brawley seismic zone, and by several small earthquakes under the Salton Sea in April 1988 (CIT/USGS catalog). Straight extrapolation of the Extra fault zone intersects the San Andreas fault at its southern terminus, where its trace is deflected into the Brawley seismic zone.

Fuis *et al.* (1984) showed a northeast-trending graben structure in their basement map, based on refraction survey data. The northwest edge of this graben coincides with the surface expression of the Extra fault zone. There had been almost no seismicity on or near this structure in the past decade or more, before the minor activity in April 1988. The Elmore Ranch fault was also seismically quiet before its 1987 activity and rupture.

We observed cracking and possibly minor left-lateral slip along a few hundred meter section of the Extra fault, just south of highway 78, following the November 1987 earthquake sequence. In 1968, following the Borrego Mountain earthquake, Clark (1972) mapped rupture on a secondary fault which may be a branch of the Extra fault. Again in 1987, cracking was observed along this secondary fault (Hudnut and Clark, 1989).

Excavations on the southern San Andreas fault have demonstrated a lack of any large earthquakes along the southern section of the San Andreas fault for the last 300 yrs (Sieh, 1986; Williams and Sieh, 1987). Since it appears that the southern San Andreas fault is in a late stage of the earthquake cycle, a decrease in normal stress on the San Andreas fault may potentially trigger a great earthquake on the Coachella Valley segment. Future studies of the Extra fault zone may assist in the evaluation of this potential.

3. Modification and Attenuation of Slip. The slip data presented in Fig. 3a and 3b show variability along strike, and our calculation of moment based on these data is nearly 10 times less than the seismic moment. These and other surface rupture data (Clark, 1972; Sharp *et al.*, 1982) indicate that large variations in slip along surface ruptures may be common. Attempts to correlate surface slip to slip at depth are an effort to match geological data with seismological and geodetic results.

In our data, two conclusions are implied: first, slip at depth was greater than surface slip—a tenth the moment and a two-fold shorter rupture length were obtained from surface rupture than from seismological data. This implies that slip is attenuated as it propagates to the surface. Second, short-wavelength variations in surface slip correspond to geological structures that are probably shallow. Evidence for this is the termination of several surface breaks at small anticlines associated with fault trace steps of less than 1 km. These structures are presumably shallow and do not continue to the basement. Fault slip is apparently modified as it propagates into these structures and to the surface—perhaps being distributed into active folding as Klinger and Rockwell (1989) have shown.

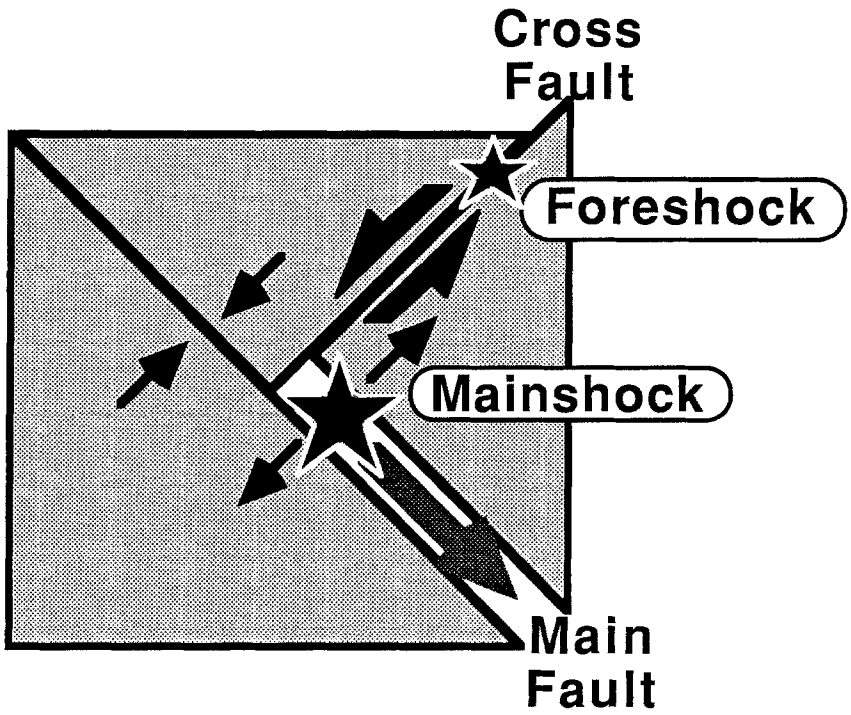

FIG. 5. Diagram of the proposed cross-fault triggering mechanism. Normal stresses on the main fault are altered by foreshock slip on cross-faults, triggering the main fault rupture near the faults' intersection. Main shock nucleates in the region of decreased normal stress and propagates southeastward, away from the region of increased normal stress. The diagram schematically represents stress changes as virtual displacements; it is not meant to be interpreted literally as actual displacements.

4. Lack of Afterslip on the Cross-Faults. If a reciprocal geometry to the foreshock/main shock triggering occurred, slip during the main shock on the Superstition Hills fault should have produced a rapid decrease in normal stress on the set of cross-faults. Suppose that slip on the cross-faults before the main shock occurred only in the basement, then a decrease in fault-normal stress on the cross-faults following the main shock allowed slip to propagate up through the sediments. This could have occurred and not been observed because of the timing of field observations. A sudden decrease in normal stress on the cross-faults accompanying the main shock might also account for the observed decrease in seismicity on these faults following the mainshock.

The greater slip at depth, shown by the seismic moment, apparently only partly propagated to the surface. Thus, some slip might still be propagating towards the surface. The above hypothesis predicts that the lack of afterslip seen through October 1988 might eventually be followed by afterslip that would be detected by future monitoring of the alinement arrays.

CONCLUSIONS

A set of parallel faults ruptured in association with the Elmore Ranch earthquake (M_S = 6.2). The ruptures occurred in a zone 10 km long and about 10 km wide along a roughly N35°E trend. Nearly 200 mm of left-lateral slip occurred across this zone, and only minor amounts of dip slip were observed. The moment obtained from surface rupture data is about an order of magnitude less than the seismic moment for this event. Seismicity indicates a 20- to 25-km-long rupture in this

event, whereas surface rupture was only half that length. No afterslip has yet been noticed on any of these surface breaks. Because these faults had left-lateral slip during the 1987 seismic events, a tectonic explanation is needed to also account for basement morphology (Fuis *et al.*, 1984), which indicates that dip slip on these faults has occurred in the past.

ACKNOWLEDGMENTS

We thank H. Kanamori and the staff at the CIT/USGS office in Pasadena, especially L. Jones and D. Given, for epicenter locations soon after the earthquakes. We also thank T. Hanks at the USGS for providing us with the new airphotos. We thank R. Sharp, M. Clark, M. Rymer, and J. Lienkaemper at the USGS, J. Kahle at CDMG, P. Williams at L-DGO/CIT, and others for their advice and comments in the field. L. Sykes pointed out the April 1988 seismicity on the Extra fault to us. Reviews by R. Wallace, C. Scholz, and D. Simpson greatly improved this paper. Research was supported by U. S. Geological Survey grant No. 14-08-00001-G1330. Lamont-Doherty Geological Observatory contribution No. 4429.

REFERENCES

Bent, A., P. Ho-Liu, and D. Helmberger (1988). The November 1987 Superstition Hills earthquake and comparisons with previous neighboring events (abstr.), *Seism. Res. Lett.* **59,** 49.

Bonilla, M. and J. Buchanan (1970). Interim report on worldwide historic surface faulting, *U.S. Geol. Surv. Open-File rept.* 32 pp.

Budding, K. E. and R. V. Sharp (1988). Surface faulting associated with the Elmore Desert Ranch and Superstition Hills, California, earthquakes of 24 November, 1987 (abstr.), *Seism. Res. Lett.* **59,** 49.

Clark, M. M. (1972). Surface rupture along the Coyote Creek fault, *U.S. Geol. Surv. Profess. Paper 787,* 55–86.

Clark, M. M. and K. Hudnut (1988). New slip along parts of the 1968 rupture of the Coyote Creek fault, California (abstr.), *Seism. Res. Lett.* **59,** 49.

Dibblee, T. W. (1984). Stratigraphy and tectonics of the San Felipe Hills, Borrego Badlands, Superstition Hills, and vicinity, in *The Imperial Basin—Tectonics Sedimentation, and Thermal Aspects: Pacific Section S.E.P.M.,* C. A. Rigsby, Editor, 31–44.

Fuis, G. S., W. D. Mooney, J. H. Healey, G. A. McMechan, and W. J. Lutter (1984). Crustal structure of the Imperial Valley region, California, in *The Imperial Basin—Tectonics, Sedimentation, and Thermal Aspects: Pacific Section S.E.P.M.,* C. A. Rigsby, Editor, 1–13.

Hudnut, K. and M. Clark (1989). New slip along parts of the 1968 Coyote Creek fault rupture, California, *Bull. Seism. Soc. Am.* **79,** 451–465.

Hudnut, K., L. Seeber, and J. Pacheco (1989). Cross-fault triggering in the November 1987 Superstition Hills earthquake sequence, southern California, *Geophys. Res. Lett.* **16,** 199–202.

Johnson, C. E. and L. K. Hutton (1982). Aftershocks and pre-earthquake seismicity, in *The Imperial Valley earthquake of October 15, 1979, U.S. Geol. Surv. Profess. Paper 1254,* 59–76.

Kahle, J. E., C. J. Wills, E. W. Hart, J. A. Treiman, R. B. Greenwood, and R. S. Kaumeyer (1988). Preliminary report: surface rupture—Superstition Hills earthquakes of November 23 and 24, 1987, *California Geology,* **41,** 4, 75–84.

Klinger, R. E. and Rockwell, T. K. (1989). Flexural-slip folding along the eastern Elmore Ranch fault in the Superstition Hills earthquake sequence of November 1987, *Bull. Seism. Soc. Am.* **79,** 297–303.

Lomnitz, C., F. Mooser, C. R. Allen, J. N. Brune, and W. Thatcher (1970). Seismicity and tectonics of the northern Gulf of California region, Mexico: preliminary results: *Geofísica Internacional* **10,** 37–48.

Magistrale, H., L. Jones, and H. Kanamori (1989). The Superstition Hills, California, earthquakes of 24 November 1987, *Bull. Seism. Soc. Am.* **79,** 239–251.

McGill, S. F., C. R. Allen, K. W. Hudnut, D. C. Johnson, W. F. Miller, and K. E. Sieh (1989). Slip on the Superstition Hills fault and on nearby faults associated with the 24 November 1987 Elmore Desert Ranch and Superstition Hills earthquakes, southern California, *Bull. Seism. Soc. Am.* **79,** 362–375.

Nicholson, C., L. Seeber, P. Williams, and L. Sykes (1986). Seismic evidence for conjugate slip and block rotation within the San Andreas fault system, southern California, *Tectonics* **5,** 4, 629–648.

Scholz, C. H. (1982). Scaling laws for large earthquakes: consequences for physical models, *Bull. Seism. Soc. Am.* **72,** 1–14.

Sharp, R. V. (1981). Variable rates of late Quaternary strike slip on the San Jacinto fault zone, southern

California, *J. Geophys. Res.* **86,** 1754–1762.

Sharp, R. V. (1989). Pre-earthquake displacement and triggered displacement on the Imperial fault associated with the Superstition Hills earthquake of 24 November 1987, *Bull. Seism. Soc. Am.* **79,** 466–479.

Sharp, R. V., K. E. Budding, J. Boatwright, M. J. Ader, M. G. Bonilla, M. M. Clark, T. E. Fumal, K. K. Harms, J. J. Lienkaemper, D. M. Morton, B. J. O'Neill, C. L. Ostergren, D. J. Ponti, M. J. Rymer, J. L. Saxton, and J. D. Sims. (1989). Surface faulting along the Superstition Hills fault zone and nearby faults associated with the earthquakes of 24 November 1987, *Bull. Seism. Soc. Am.* **79,** 252–281.

Sharp, R. V., J. Lienkaemper, M. Bonilla, D. Burke, B. Fox, D. Herd, D. Miller, D. Morton, D. Ponti, M. Rymer, J. Tinsley, J. Yount, J. Kahle, E. Hart, and K. Sieh (1982). Surface faulting in the central Imperial Valley, *U.S. Geol. Surv. Profess. Paper 1254*, 119–143.

Sieh, K. E. (1986). Slip rate across the San Andreas fault and pre-historic earthquakes at Indio, California, *EOS* **67,** 1200.

Slemmons, D. B. (1977). State of the art for assessing earthquake hazards in the U.S., faults and earthquake magnitudes, U.S. Army Eng. Waterway Exp. Sta., Vicksburg, Mississippi, 229.

Williams, P. L. and H. W. Magistrale (1989). Slip along the Superstition Hills fault associated with the 24 November 1987 Superstition Hills, California, earthquake, *Bull. Seism. Soc. Am.* **79,** 390–410.

Williams, P. and K. E. Sieh (1987). Decreasing activity of the southernmost San Andreas fault during the past millenium, *Geol. Soc. Am. Abstracts with Programs* **19,** 891.

LAMONT-DOHERTY GEOLOGICAL OBSERVATORY
PALISADES, NEW YORK 10964
(K.W.H., L.S.)

DEPARTMENT OF GEOLOGICAL SCIENCES
SAN DIEGO STATE UNIVERSITY
SAN DIEGO, CALIFORNIA 92182
(T.R., J.G., R.K., S.L., R.M.)

DEPARTMENT OF GEOLOGICAL SCIENCES
COLUMBIA UNIVERSITY
NEW YORK, NEW YORK 10027
(K.W.H.)

Manuscript received 28 July 1988